8-2006

Scanning Electrochemical Mapping of Spatially Localized Electrochemical Reactions Induced by Surface Potential Gradients

Shrisudersan Jayaraman
Iowa State University

Erin L. May
Iowa State University

Andrew C. Hillier
Iowa State University, hillier@iastate.edu

Scanning Electrochemical Mapping of Spatially Localized Electrochemical Reactions Induced by Surface Potential Gradients†

Shrisudersan Jayaraman,‡ Erin L. May, and Andrew C. Hillier*

Department of Chemical and Biological Engineering and Department of Chemistry, Iowa State University, Ames, Iowa 50011

Received March 15, 2006. In Final Form: May 24, 2006

The influence of a surface potential gradient on the location and extent of electrochemical reactions was examined using a scanning electrochemical microscope. A linear potential gradient was imposed on the surface of a platinum-coated indium tin oxide electrode by applying two different potential values at the edges of the electrode. The applied potentials were used to control the location and extent of several electrochemical reactions, including the oxidation of $Ru(NH_3)_6^{2+}$, the oxidation of H_2, and the oxidation of H_2 in the presence of adsorbed CO. Scanning electrochemical mapping of these reactions was achieved by probing the feedback current associated with the oxidation products. The oxidation of $Ru(NH_3)_6^{2+}$ occurred at locations where the applied potential was positive of the formal potential of the $Ru(NH_3)_6^{2+/3+}$ redox couple. The position of this reaction on the surface could be spatially translated by manipulating the terminal potentials. The rate of hydrogen oxidation on the platinum-coated electrode varied spatially in the presence of a potential gradient and correlated with the nature of the electrode surface. High oxidation rates occurred at low potentials, with decreasing rates observed as the potential increased to values where platinum oxides formed. The extent of oxide formation versus position was confirmed with in-situ ellipsometry mapping. In the presence of adsorbed carbon monoxide, a potential gradient created a localized region of high activity for hydrogen oxidation at potentials between where carbon monoxide was adsorbed and platinum oxides formed. The position of this localized region of activity could be readily translated along the surface by changing the terminal potential values. The ability to manipulate electrochemical reactions spatially on a surface has potential application in microscale analytical devices as well as in the discovery and analysis of electrocatalytic systems.

Introduction

There has been increasing interest in the development and use of well-defined surface gradients for the construction of materials with tailored and spatially controllable properties,[1,2] for the design of dense combinatorial libraries,[3] and for novel analytical testing methods.[4] Surface composition gradients have been used to control local wettability[5] as well as to study cell and protein interactions with surfaces.[6−8] Temperature gradients have been used in the construction of combinatorial polymer libraries.[9] Gradients have also been used for inducing motion in liquid drops,[5] demixing in lipid bilayer membranes,[10] control of liquid crystal orientation,[11] and spatial control of electrochemical reactions.[12,13] The construction of combinatorial libraries and the development of high-throughput testing methods have exploited gradients to examine polymer thin-film dewetting,[14] to construct phase diagrams,[9] to study mushroom-to-brush crossover in surface-anchored polyacrylamide films,[15] and to perform coverage and composition-dependent reactivity mapping of heterogeneous catalysts.[13,16]

A variety of methods have been used for the construction of surface gradients, including free diffusion,[5−7] diffusion in microfluidic networks,[17] STM-based replacement lithography,[18] physical vapor deposition,[6,11] and imposed electrochemical[12,13] or electric field gradients.[10,19] Electrochemical gradients represent a novel method for the construction of surface gradients as well as for the local control of electrode surfaces. Electrochemical gradients are particularly appealing because of both the flexibility and reversibility of control that they provide. Electrochemical gradients have been used to fabricate self-assembled monolayer gradients,[12,20,21] gradients in electrodeposited polymers,[22] model surfaces for cell and protein adhesion studies,[23−25] composition gradients of various metals,[13,16,26,27] and spatially controllable pH gradients.[28]

† Part of the Electrochemistry special issue.

* Corresponding author. E-mail: hillier@iastate.edu. Phone: (515) 294-3678. Fax: (515) 294-2689.

‡ Current address: Corning Inc., 1 Science Center Drive, Corning, New York 14831.

(1) Rawlings, R. *Mater. World* **1995**, *3*, 474.
(2) Marple, B. R.; Boulanger, J. *J. Am. Ceram. Soc.* **1994**, *77*, 2747.
(3) Xiang, X.-D.; Sun, X.; Briceno, G.; Lou, Y.; Wang, K.-A.; Chang, H.; Wallace-Freedman, W. G.; Chen, S.-W.; Schultz, P. G. *Science* **1995**, *268*, 1738.
(4) Neubrand, A.; Rodel, J. *Z. Metallkd.* **1997**, *88*, 358.
(5) Chaudhury, M. K.; Whitesides, G. M. *Science* **1992**, *256*, 1539.
(6) Ruardy, T. G.; Schakenraad, J. M.; van der Mei, H. C.; Busscher, H. J. *Surf. Sci. Rep.* **1997**, *29*, 3.
(7) Elwing, H.; Gölander, C. G. *Adv. Colloid Interface Sci.* **1990**, *32*, 317.
(8) Mougin, K.; Ham, A. S.; Lawrence, M. B.; Fernandez, E. J.; Hillier, A. C. *Langmuir* **2005**, *21*, 4809.
(9) Meredith, J. C.; Karim, A.; Amis, E. J. *Macromolecules* **2000**, *33*, 5760.
(10) Groves, J. T.; Boxer, S. G.; McConnell, H. M. *Proc. Natl. Acad. Sci. U.S.A.* **1998**, *95*, 935.
(11) Tingey, M. L.; Luk, Y. Y.; Abbott, N. L. *Adv. Mater.* **2002**, *14*, 1224.
(12) Balss, K. M.; Coleman, B. D.; Lansford, C. H.; Haasch, R. T.; Bohn, P. W. *J. Phys. Chem. B* **2001**, *105*, 8970.
(13) Jayaraman, S.; Hillier, A. C. *Langmuir* **2001**, *17*, 7857.
(14) Meredith, J. C.; Smith, A. P.; Karim, A.; Amis, E. J. *Macromolecules* **2000**, *33*, 9747.
(15) Wu, T.; Efimenko, K.; Genzer, J. *J. Am. Chem. Soc.* **2002**, *124*, 9394.
(16) Jayaraman, S.; Hillier, A. C. *Meas. Sci. Technol.* **2005**, *16*, 5.
(17) Dertinger, S. K. W.; Chiu, D. T.; Jeon, N. L.; Whitesides, G. M. *Anal. Chem.* **2001**, *73*, 1240.
(18) Fuierer, R. R.; Carroll, R. L.; Feldheim, D. L.; Gorman, C. B. *Adv. Mater.* **2002**, *14*, 154.
(19) Lee, K. Y. C.; Klingler, J. F.; McConnell, H. M. *Science* **1994**, *263*, 655.
(20) Balss, K. M.; Fried, G. A.; Bohn, P. W. *J. Electrochem. Soc.* **2002**, *149*, C450.
(21) Balss, K. M.; Kuo, T. C.; Bohn, P. W. *J. Phys. Chem. B* **2003**, *107*, 994.
(22) Wang, X. J.; Bohn, P. W. *J. Am. Chem. Soc.* **2004**, *126*, 6825.
(23) Plummer, S. T.; Wang, Q.; Bohn, P. W.; Stockton, R.; Schwartz, M. A. *Langmuir* **2003**, *19*, 7528.
(24) Wang, Q.; Bohn, P. W. *J. Phys. Chem. B* **2003**, *107*, 12578.
(25) Wang, Q.; Jakubowski, J. A.; Sweedler, J. V.; Bohn, P. W. *Anal. Chem.* **2004**, *76*, 1.
(26) Coleman, B. D.; Finnegan, N.; Bohn, P. W. *J. Electroanal. Chem.* **2004**, *571*, 139.
(27) Coleman, B. D.; Finnegan, N.; Bohn, P. W. *Thin Solid Films* **2004**, *467*, 121.

10.1021/la0607048 CCC: $33.50
Published on Web 08/03/2006

Scheme 1. Schematic of the Sample Used for SECM Mapping of the Surface Potential Gradient

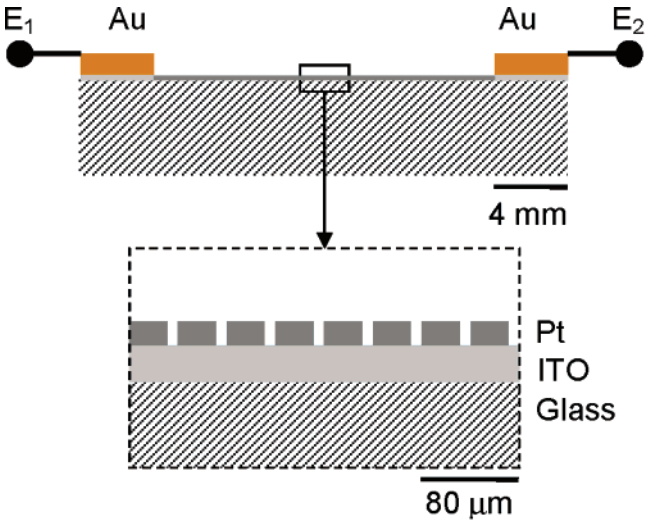

In this work, we demonstrate the ability of an applied potential gradient to control the extent and spatial position of several electrochemical reactions and spatially map these processes using a scanning electrochemical microscope (SECM). SECM was employed to directly quantify the magnitude and spatial extent of electrochemical reactions on a platinum-coated electrode in the presence of various potential gradients. The influence of a surface potential gradient on the behavior of a simple redox reaction involving the $Ru(NH_3)_6^{2+/3+}$ couple was examined. In addition, the influence of a potential gradient on local electrocatalytic activity for the hydrogen oxidation reaction was explored. The impact of a potential gradient on oxide formation and carbon monoxide adsorption on platinum were both examined in terms of their influence on the magnitude and spatial position of the hydrogen oxidation reaction. We demonstrate the ability to adjust the position of these features readily on an electrode surface by controlling the magnitude and extent of the applied potential gradient.

Experimental Methods

Materials and Reagents. All experiments were performed in 18 MΩ deionized water (E-Pure, Barnstead, Dubuque, IA). Electrochemical measurements were performed in solutions containing as-received ruthenium hexamine ($Ru(NH_3)_6Cl_3$), sulfuric acid (H_2SO_4), and sodium sulfate (Na_2SO_4) (Aldrich, Milwaukee, WI). Unless otherwise noted, the solutions were deaerated with nitrogen (BOC Gases, Murray Hill, NJ) prior to each measurement. Carbon monoxide-coated surfaces were created by delivering pure CO gas (BOC Gases, Murray Hill, NJ) to the electrochemical apparatus by bubbling through a porous ceramic frit (Ace Glass, Inc., Vineland, NJ) into the electrolyte solution for a period of 5 min with the working electrode held at a potential of 0.1 V. The CO was then removed from solution by purging with nitrogen for a period of 15 min. Deposits of Pt were obtained by electrodeposition (vide infra) from solutions containing 1−10 mM chloroplatinic acid (H_2PtCl_6) (Strem Chemicals, Newburyport, MA) in 0.1 M Na_2SO_4.

Substrate Fabrication. Indium tin oxide (ITO)-coated glass slides (Delta Technologies, Stillwater, MN) with a surface resistance of $R_s \approx 100\ \Omega$ square^{-1} were cut to a size of 25 × 25 mm^2 and then patterned with bands of Pt to create the final sample configuration used for SECM imaging (Scheme 1). The band pattern was fabricated in order to avoid generating a continuous Pt film on the ITO surface. A continuous metallic film could decrease the resistance of the sample to the point where the potentiostat was unable to drive enough current through the electrode to maintain the linear potential gradient. Using a band pattern ensured that the resistance of the sample maintained the value of the ITO substrate.

The ITO was patterned using photolithography to fabricate a series of bands with a length of 25 mm and a width of ∼30 μm, separated by ∼10-μm-wide strips of photoresist. To make this pattern, a thin layer of the photoresist (Microposit S1813 Photoresist, Shipley, Marlborough, MA) was coated on the ITO substrate by spin coating at 1000 rpm for 30 s. Subsequently, the substrate was soft-baked in a convection oven at 100° C for 30 min. The substrate was then exposed to ultraviolet light for 15 min through a patterned mask (Ronchi slide, Edmund Industrial Optics, Barrington, NJ). The substrate was developed immediately (Microposit MF-319 Developer, Shipley, Marlborough, MA), leaving behind the unexposed photoresist with the desired pattern. Finally, the sample was hard baked at 110° C for 30 min.

Platinum was electrodeposited onto the exposed ITO bands to form a thin coating from a solution of 10 mM $H_2PtCl_6{\cdot}6H_2O$ and 0.1 M Na_2SO_4 using a potentiostat (model CH1030, CH Instruments Inc., Austin, TX). A square wave potential program with limits of 0 and −1.5 V (vs Hg/Hg_2SO_4) at a frequency of 100 Hz was applied for 2 min to create a uniform coating of platinum. After electrodeposition, the photoresist was stripped from the surface by immersing the substrate in photoresist remover (Microposit Remover 1165, Shipley, Marlborough, MA) for ∼2 min. This procedure produced 30-μm-wide platinum bands separated by 10 μm strips of ITO. The substrate was cleaned thoroughly with deionized water before performing any further experiments. Electrical contact pads were then fabricated onto the ends of the platinum-coated ITO regions by depositing gold through a mask that exposed the edges of the sample. Approximately 100 nm of gold was vapor deposited (Denton Vacuum Turbo III, Moorestown, NJ) onto the ends of the substrate at a pressure of $\sim 7 \times 10^{-5}$ Torr at a rate of 1 to 2 Å s^{-1}. Electrical contact was achieved by attaching a copper wire to the gold contact pads using a conductive silver epoxy (H20E, Epoxy Technologies, Billerica, MA), followed by an insulating epoxy (QuickSet Epoxy Gel, Hentel Consumer Adhesives Inc., Avon, OH).

Electrochemistry and Scanning Electrochemical Microscopy. The scanning electrochemical microscope (SECM) used in this work was a custom-built model similar to that described in the literature,[29,30] with a slight modification of the electronics to allow for the electric field gradients to be applied. Briefly, the positioning system consisted of a motor driver (UNIDRIV6000, Newport Corporation, Irvine, CA) connected to three integrated stepper motor/linear translation stages (ILS Series, Newport Corporation, Irvine, CA) assembled in an orthogonal fashion to provide three independent directions of motion. The motor driver was interfaced via a motion controller card (ESP6000, Newport Corporation, Irvine, CA) to a personal computer. The sample platform consisted of an optical table (Newport Corporation, Irvine, CA) with a custom-built Teflon cell mounted on a multiaxis tilt stage (model 39, Newport, Irvine, CA). Electrochemical measurements were performed with two bipotentiostats (model AFRDE, PINE Instrument Company, Grove City, PA) connected in such a way that three working electrodes could be controlled in combination with a single reference and counter electrode. Two of these electrodes were used to control the substrate potentials (E_1 and E_2), and the third controlled the potential of the tip electrode (E_{tip}). Details of the potentiostat connections and a block circuit diagram are provided in Supporting Information. One bipotentiostat was used to impose the electric field gradient at the substrate surface, and the other was used to control the potential of the scanning tip. Common reference and counter electrodes were used for both bipotentiostats. The reference electrode was a Hg/Hg_2SO_4 electrode, but all potential values are reported with respect to the reversible hydrogen electrode (RHE). SECM tips were fabricated with 25-μm-diameter gold wires (Goodfellow, Berwyn, PA) sealed in glass using a technique similar to that described in

(28) May, E. L.; Hillier, A. C. *Anal. Chem.* **2005**, *77*, 6487.

(29) Bard, A. J.; Fan, F.-R. F.; Pierce, D. T.; Unwin, P. R.; Wipf, D. O.; Zhou, F. *Science* **1991**, *254*, 68.

(30) Kwak, J.; Bard, A. J. *Anal. Chem.* **1989**, *61*, 1794.

the literature.[31] The tip current was measured with a high-sensitivity current amplifier (Keithley Instruments, Inc., Cleveland, OH) and recorded using a multifunction data acquisition board (model NI 6036E, National Instruments, Austin, TX). Tip positioning and data acquisition were performed with a custom-designed scanning program written in LabView (National Instruments, Austin, TX).

Ellipsometry. An in-situ ellipsometry cell was fabricated from a piece of Delrin and glass microscope slides. A $7.5 \times 5.1 \times 1$ cm^3 piece of Delrin was machined along two parallel sides at 20°. Glass slides were glued (QuickTite Super Glue, Manco, Inc., Avon, OH) to the Delrin to provide optical access to the sample at a 70° angle of incidence. Two more glass slides were adhered to the remaining ends to create a closed cell. The cell wall joints were then covered with an inert organic lacquer (Microstop stop-off lacquer, Pyramid Plastics Inc., Hope, AR). For ellipsometry measurements, the substrate consisted of a layer of platinum electrodeposited between gold contact pads on an ITO substrate. The band structure as described earlier was not used in these samples. Electrical contact to the substrates was achieved by attaching a copper wire to the gold contact pads using a conductive silver epoxy (H20E, Epoxy Technologies, Billerica, MA), followed by an insulating epoxy (QuickSet Epoxy Gel, Hentel Consumer Adhesives Inc., Avon, OH). The gold contact pads, epoxy, and copper wires were coated in the organic lacquer to isolate them from solution. Hg/Hg_2SO_4 reference and Pt/Ir counter electrodes were suspended in the cell for potential control. Experiments were performed in a solution of 0.1 M Na_2SO_4 and 5 mM H_2SO_4.

Null-ellipsometry measurements were performed using an automated, multifunctional optical system (Multiskop, Optrel GbR, Berlin, Germany) with spatial mapping capabilities. Ellipsometric data were acquired at a single wavelength (632.8 nm) with a beam diameter of ~0.6 mm in the PCSA configuration at a 70° angle of incidence. Film calculations were performed using a commercial software package (Elli, Optrel GbR, Berlin, Germany). The refractive index, n, and absorption coefficient, k, of the substrate ($n = 2.062$, $k = -0.860$) were determined using a two-phase model (water/substrate) at a potential of 0.0 V (vs NHE). The absorption coefficient used here varies from that observed for bulk Pt electrodes ($k = -4.6$).[32] This difference is most likely due to the semitransparent nature of our Pt-coated ITO film. The thickness of the platinum oxide film was then calculated as a function of applied potential using a three-phase model (water/film/substrate) and estimated optical constants ($n = 2.8$, $k = -0.3$). Ellipsometry mapping experiments were performed by translating the sample along the direction of the applied potential gradient using an integrated stepper motor and recording delta and psi with a uniform potential of 0 V and in the presence of an applied potential gradient. The *changes* in delta and psi at each position were used to determine the oxide thickness.

Results and Discussion

Cyclic voltammetry of a platinum-coated indium tin oxide (ITO) electrode in a solution of 5 mM $Ru(NH_3)_6Cl_3$/0.1 M Na_2SO_4 (Figure 1a) exhibits the typical response for a reversible redox reaction.[33] The formal potential for the $Ru(NH_3)_6^{3+\backslash 2+}$ couple is ~0.25 V versus RHE. At potentials negative of this value, $Ru(NH_3)_6^{3+}$ in solution is reduced, whereas at potentials positive of this value, $Ru(NH_3)_6^{2+}$ near the electrode surface is oxidized. Under normal conditions, these reactions would occur uniformly over the entire electrode surface at a rate dictated by the applied electrode potential. In the presence of a surface electric field gradient, however, the rates of these reactions vary spatially along the surface. Evidence of the magnitude and extent of these spatially varying reaction rates can be visualized through several methods, such as the formation of surface films,[27] the evolution or consumption of chemical species at the electrode surface, or optical methods such as surface plasmon resonance (SPR)[12] or surface-enhanced Raman spectroscopy (SERS).[21] Scanning electrochemical microscopy (SECM) represents a high-resolution electrochemical mapping strategy that can also be employed to quantify these spatially varying electrochemical processes directly.[31]

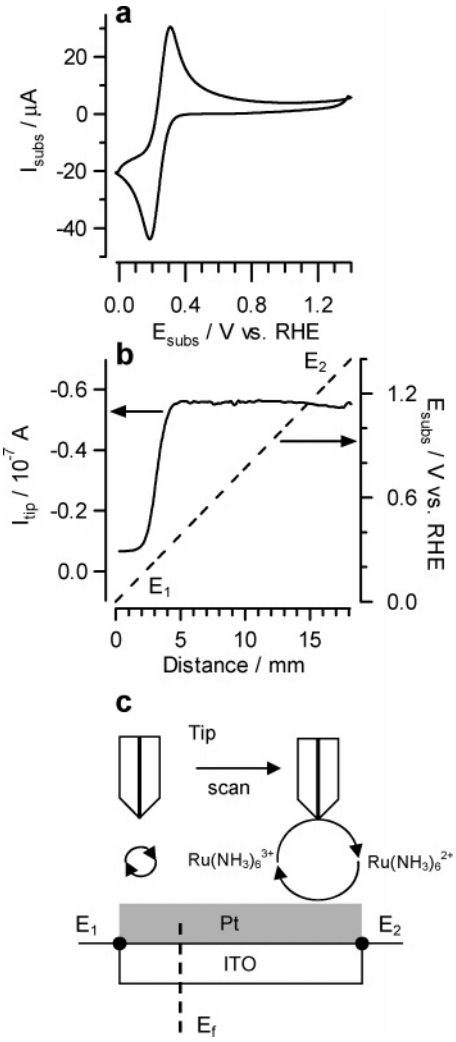

Figure 1. (a) Cyclic voltammogram of a Pt-coated ITO electrode in a nitrogen-purged solution containing 5 mM $Ru(NH_3)_6Cl_3$/0.1 M Na_2SO_4. (b) SECM line scan (−) and substrate potential (- -) along the electrode surface. The substrate potentials are $E_1 = 0$ V and $E_2 = 1.4$ V while the tip is held at $E_{tip} = -0.15$ V where the diffusion-limited reduction of $Ru(NH_3)^{3+}$ occurs. (c) Schematic of the tip−substrate interface showing electrochemical reactions at the tip and substrate (magnitude of reaction indicated by size of arrows) vs applied potential. The approximate location of the formal potential (E_f) for $Ru(NH_3)^{3+/2+}$ is shown.

Figure 1b depicts the results of an SECM mapping experiment in which a linear potential gradient is applied along the electrode surface in the presence of 5 mM $Ru(NH_3)_6^{3+}$. Terminal potential values of $E_1 = 0.0$ V and $E_2 = 1.4$ V are applied to create a gradient with a 1.4 V change over a distance of ~18 mm. Under these conditions, the left side of the substrate near E_1 presents potential values sufficient to reduce $Ru(NH_3)_6^{3+}$ in solution whereas the right side near E_2 oxidizes $Ru(NH_3)_6^{2+}$. During SECM mapping experiments, the tip potential is held at $E_{tip} = -0.15$ V, where the diffusion-limited reduction of $Ru(NH_3)_6^{3+}$ occurs at the tip with a current of $I_{tip,inf} \approx -27$ nA. A scan over the substrate at a tip−substrate separation of ~5 μm produces a nonuniform tip current that varies between high and low current

(31) Shah, B. C.; Hillier, A. C. *J. Electrochem. Soc.* **2000**, *147*, 23.
(32) Kim, S. H.; Paik, W. K.; Bockris, J. O. *Surf. Sci.* **1972**, *33*, 617.
(33) Bard, A. J.; Faulkner, L. R. *Electrochemical Methods: Fundamentals and Applications*, 2nd ed.; John Wiley: New York, 2001.

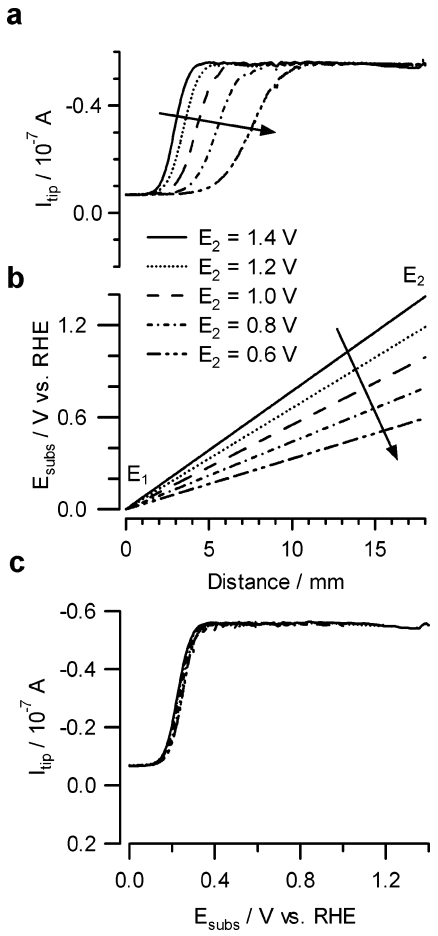

Figure 2. (a) SECM line scans and (b) applied substrate potentials vs position along a Pt-coated ITO electrode showing the influence of changing E_2 on the electrode response. The potential gradients range from $E_1 = 0$ V on the left to E_2 on the right with values that include $E_2 = 1.4$ V (−), 1.2 V (••), 1.0 V (- -), 0.8 V (-•-), and 0.6 V (-•••-). The tip is held at $E_{tip} = -0.15$ V, and the solution contains 5 mM $Ru(NH_3)_6Cl_3$/0.1 M Na_2SO_4. (c) Overlay of SECM line scans plotted as tip current vs substrate potential.

values. At substrate positions between 5 and 18 mm, the tip current is large and reflects a large positive feedback between the tip and substrate ($I_{tip} \approx 60$ nA). At these locations, the substrate potential is above the $Ru(NH_3)_6^{3+/2+}$ formal potential, so $Ru(NH_3)_6^{3+}$ that is reduced to $Ru(NH_3)_6^{2+}$ at the tip diffuses to the substrate and is oxidized back to $Ru(NH_3)_6^{3+}$. This positive feedback between tip and substrate reflects a large substrate oxidation rate. With further scanning, the tip current decreases rapidly at a position of ~3 mm. This decrease in tip current occurs at a substrate position that coincides with the formal potential of the $Ru(NH_3)_6^{3+/2+}$ couple. At locations to the left of this position, the tip current maintains a steady, low value ($I_{tip} \approx$ 5nA) as the substrate shields the tip and also reduces $Ru(NH_3)_6^{3+}$ in solution, which limits its availability to the SECM tip. A schematic of the tip−substrate interface depicting the geometry and the magnitudes of the reactions occurring in the tip−substrate gap during this experiment are depicted in Figure 1c. The feedback current is large on the right side of the sample where the potential is above that for the $Ru(NH_3)_6^{3+/2+}$ couple and low on the left side where the potential is below this value.

The extent and spatial location of the $Ru(NH_3)_6^{3+/2+}$ reaction on the surface is readily manipulated by changing the values of the terminal potentials. In Figure 2, a series of SECM line scans were acquired for different values of the terminal potential E_2. With a value of $E_2 = 1.4$ V, the SECM line scan (Figure 2a) shows a transition from positive to negative feedback near ~3 mm, which is consistent with the location of the formal potential for the $Ru(NH_3)_6^{3+/2+}$ reaction on the surface. Decreasing the magnitude of E_2 produces a shallower potential gradient (Figure 2b) and moves the transition in tip current to the right. As E_2 is decreased further from 1.4 down to 0.6 V in increments of 0.2 V, SECM line scans show that the location of the transition in tip current shifts further to the right along the surface. Thus, by simply changing the value of the terminal potentials, the position of the electrochemical reaction on the surface can be readily manipulated. Notably, the curves for all five potential gradients coincide if plotted as tip current versus substrate potential (Figure 2c).

This simple electron-transfer reaction involving $Ru(NH_3)_6^{3+/2+}$ exhibits a reaction rate that is not sensitive to the nature of the electrode surface. However, a catalytic reaction such as the oxidation of H_2 involves an adsorption step on platinum that is highly sensitive to the nature of the surface as well as the presence of platinum oxides.[34−36] This reaction can be readily monitored with the SECM by using the reduction of protons as the tip reaction. A tip potential of $E_{tip} = -1.0$ V was used to monitor this reaction. This large negative potential was used to ensure that our gold microelectrode tip reached the diffusion-limited plateau current for proton reduction, which gave an infinity current of $I_{tip,inf} \approx -130$ nA. With this tip reaction, proton reduction at the tip electrode produces hydrogen gas, which can diffuse and oxidize at the substrate. The protons produced at the substrate can then diffuse back to the tip and produce feedback current, which can be used as a measure of the magnitude of the hydrogen oxidation rate at the substrate. This technique has been employed to characterize catalyst electrodes as well as to perform combinatorial screening experiments for fuel cell catalysts.[16,37,38]

Cyclic voltammetry of a platinum-coated ITO electrode in a solution of 5 mM H_2SO_4/0.1 M Na_2SO_4 displays the features typical of platinum in an acidic solution (Figure 3a). Hydrogen underpotential deposition (UPD) peaks are evident at potentials just positive of 0 V. Oxide formation is indicated by the broad oxidation at more positive electrode potentials and by the symmetric reduction peak in the reverse scan. Platinum oxides would be expected to appear as the potential approaches and exceeds ~0.6 V. An SECM line scan across the substrate electrode at a tip−substrate separation of ~10 μm with constant terminal potential values of $E_1 = E_2 = 0.1$ V (Figure 3b) shows uniformly large feedback at the tip, which indicates a large and uniform hydrogen oxidation rate across the substrate. In the presence of a surface potential gradient, the behavior is significantly different. Terminal potential values of $E_1 = 0.0$ V and $E_2 = 1.4$ V (Figure 3c) produce a potential gradient that spans the range of surface behavior indicated in Figure 3a. In this case, the SECM line scan shows a large feedback current, indicating a high substrate reaction rate, on the left side of the sample. As the tip moves across the sample to increasing substrate potential values, the feedback current decreases continuously, starting near ~8 mm, which corresponds to a surface potential value of ~0.6 V, until it plateaus at a minimum value at ~16 mm with a potential >1.2 V. A schematic of the tip−sample interface (Figure 3d) suggests that the potential-dependent formation of platinum oxides on the

(34) Frumkin, A.; Sobol, V.; Dmitrieva, A. *J. Electroanal. Chem.* **1967**, *13*, 179.
(35) Schuldiner, S. *J. Electrochem. Soc.* **1968**, 362.
(36) Markovic, N. M.; Grgur, B. N.; Ross, P. N. *J. Phys. Chem. B* **1997**, *101*, 5405.
(37) Fernandez, J. L.; Walsh, D. A.; Bard, A. J. *J. Am. Chem. Soc.* **2005**, *127*, 357.
(38) Fernandez, J. L.; Bard, A. J. *Anal. Chem.* **2003**, *75*, 2967.

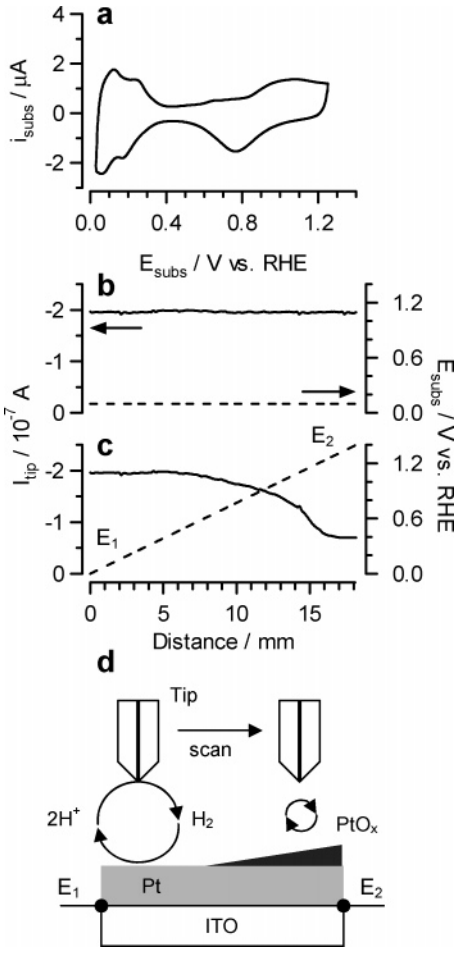

Figure 3. (a) Cyclic voltammogram of Pt-coated ITO in a nitrogen-purged solution containing 5 mM H_2SO_4/0.1 M Na_2SO_4. SECM line scans and potential profiles for (b) $E_1 = E_2 = 0.1$ V and (c) $E_1 = 0$ V and $E_2 = 1.4$ V showing the tip current (−) and substrate potential (- -). The tip potential is held at −1.0 V such that the diffusion-limited reduction of protons occurs. (d) Schematic of tip−substrate interface corresponding to the results in part c showing tip and substrate reactions and the potential-dependent formation of platinum oxide (PtO_x) on the surface. The magnitude of the reaction rate is indicated by the size of the arrows.

surface causes the decrease in the hydrogen oxidation rate observed in the presence of a potential gradient.

To quantitatively compare the SECM line scan results with electrochemically induced changes in the substrate electrode, in-situ ellipsometry measurements were performed. Figure 4 depicts null ellipsometry results for an electrodeposited platinum film on ITO while being cycled between 0 and 1.4 V (vs NHE) in a solution of 5 mM H_2SO_4/0.1 M Na_2SO_4. Figure 4a shows the change in delta as a function of applied potential, and Figure 4b shows the change in psi. During the forward potential scan, delta decreases gradually between 0.0 and 0.8 V and then decreases rapidly with further increasing potential. Psi, in contrast, increases steadily over the same range in potential. The decrease in delta of approximately 4° suggests the formation of an oxide film.[39] The changes appear at potentials consistent with the oxidation current observed in cyclic voltammetry (Figure 3a). During the return sweep in potential from 1.4 to 0 V, delta increases while psi decreases until they reach their original values at 0.0 V. In both, a rapid change is observed at a potential corresponding to the oxide reduction peak in Figure 3a.

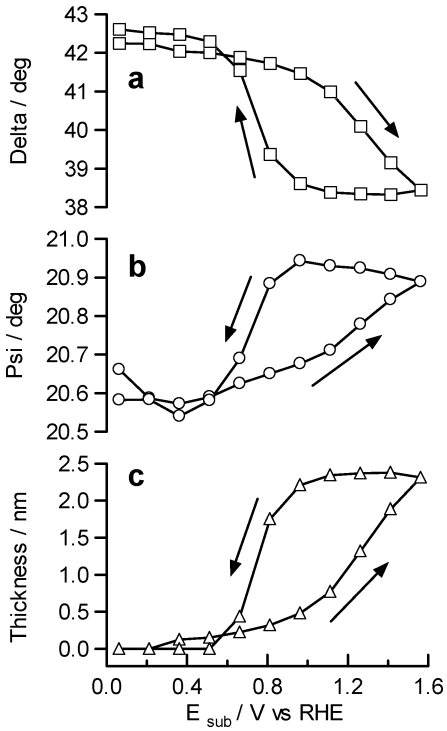

Figure 4. Potential-dependent null ellipsometry on a platinum-coated ITO surface showing (a) delta (□) and (b) psi (○) vs applied potential. (c) Plot of oxide thickness vs potential (△) as determined by fitting potential-dependent ellipsometry results to the three-layer model.

Previously, ellipsometric measurements on bulk platinum electrodes indicated that changes in delta and psi could be used to deduce the potential-dependent thickness of a growing oxide film.[32,40] To convert the changes in delta and psi measured here to an estimate of the oxide thickness, a three-layer optical model (water−oxide−substrate) was used. Optical constants for the platinum-coated ITO substrate were first determined at a potential of 0.0 V ($n = 2.062$ and $k = -0.860$). The changes in delta and psi were then fit to a three-layer model using estimated optical constants for the oxide ($n = 2.8$, $k = -0.3$) to determine the thickness of the oxide film. Results of this fitting procedure (Figure 4c) indicate a slow film growth starting at ∼0.6 V and then a rapid increase in thickness to a maximum of ∼2.3 nm near 1.6 V. During the reverse scan, the oxide film is removed rapidly as the potential decreases below ∼0.8 V. The potentials at which the oxide film forms and is removed are consistent with the cyclic voltammetry shown in Figure 3a. Notably, the oxide thickness observed here is somewhat larger than that reported for short-timescale oxide growth on bulk Pt electrodes.[32,40] This difference in measured oxide thickness could be influenced by the timescale of the experiments as well as the nature of the electrodes examined.

To quantify the nature of the oxide film formed in the presence of a surface potential gradient, null-ellipsometry mapping experiments were performed. A platinum-coated ITO electrode was prepared, and in-situ ellipsometry mapping was performed along the surface in the presence of a linear potential gradient. Because small variations in the quality of the substrate resulted in changes in the measured optical constants whose values exceeded those induced by an applied potential, the ellipsometry results are reported as the changes in delta and psi at each location. These changes refer to those measured in the presence of the

(39) Gottesfeld, S. *Electroanaly. Chem.* **1989**, *15*, 143.

(40) Reddy, A. K. N.; Genshaw, M. A.; Bockris, J. O. *J. Chem. Phys.* **1968**, *48*, 671.

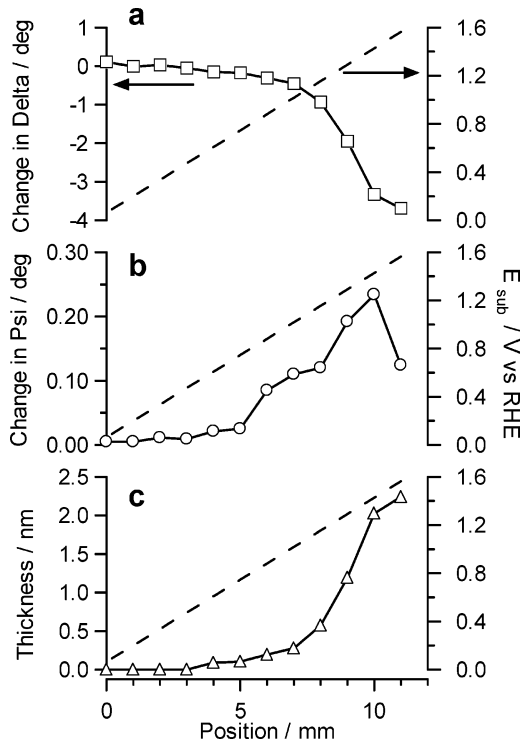

Figure 5. Position-dependent null ellipsometry on a platinum-coated ITO surface in the presence of an applied potential gradient. (a) Change in delta (□), (b) change in psi (○), and (c) oxide thickness (△) vs position with an applied potential gradient between 0 and 1.6 V (- -) over a region spanning 0 to 12 mm.

surface potential gradient with respect to the same locations measured with a uniform potential of 0.0 V. Changes in delta (Figure 5a) and psi (Figure 5b) were monitored with respect to electrode position for a surface potential gradient spanning 0.0 to 1.6 V. The observed changes in these parameters are consistent with those observed at a fixed location during potential cycling. As the potential increases along the gradient from the left to the right of the sample, delta decreases gradually at first and then more rapidly as the potential reaches and exceeds ~0.6 V (Figure 5a). Similarly, psi increases gradually at low potentials on the left and then more rapidly at higher potentials on the right (Figure 5b). The only anomalous result appears to be the psi value measured at the far right side of the sample. The lower value measured here could be due to overlap with the gold contact pad at this location. Nevertheless, the thickness of the oxide layer could be determined as a function of position in the presence of the potential gradient from these results using a three-layer model (Figure 5c). The thickness of the oxide layer versus position and potential is consistent with that observed in the potential cycling results. A variation in oxide thickness between 0 and ~2.3 nm is observed along the gradient. As suggested in the previous Figures, the decrease in feedback current for hydrogen oxidation correlates with the increase in oxide layer thickness. This is consistent with the blocking behavior of oxide films observed during oxygen evolution on platinum surfaces.[41]

In addition to oxide formation, another species that dramatically alters the catalytic activity of platinum toward hydrogen oxidation is carbon monoxide.[42,43] Carbon monoxide strongly adsorbs to platinum to block active sites and poison the surface. The impact

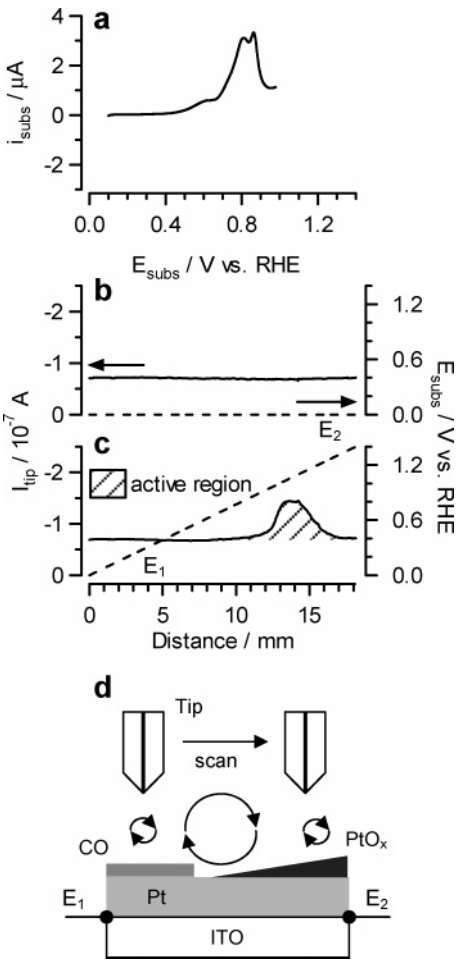

Figure 6. (a) Cyclic voltammogram of a Pt-coated ITO in a carbon monoxide-purged solution containing 5 mM H_2SO_4/0.1 M Na_2SO_4. SECM line scans and potential profiles for (b) $E_1 = E_2 = 0.1$ V and (c) $E_1 = 0$ V and $E_2 = 1.4$ V showing the tip current (−) and substrate potential (- -). The tip potential is held at −1.0 V such that the diffusion-limited reduction of protons occurs. The active region between CO and oxide-covered surface regions is indicated by the hatched pattern. (d) Schematic of the tip−substrate interface corresponding to the results in part c showing reactions and surface regions covered with carbon monoxide (CO) and platinum oxide (PtO_x). The magnitude of the reaction rate is indicated by the size of the arrows.

of carbon monoxide adsorption can be readily seen from Figure 6a, which depicts a linear sweep voltammogram for a platinum-coated ITO electrode after exposure to carbon monoxide in a solution of 5 mM H_2SO_4/0.1 M Na_2SO_4. A comparison of this result to Figure 3a shows the absence of hydrogen adsorption peaks at low potentials due to the blocking effect of carbon monoxide. In addition, a large anodic peak appears at ~0.8 V. This peak reflects the oxidation of carbon monoxide from the electrode surface, which occurs at a potential just preceding the formation of platinum oxides.

The impact of adsorbed carbon monoxide on the hydrogen oxidation reaction is to lower the reaction rate drastically. This can be visualized by a line scan with the SECM over the Pt electrode with the surface held at a uniform potential of 0.0 V (Figure 6b). At this potential, the surface is completely blocked by a layer of carbon monoxide, and the tip current is uniformly low over the entire surface, in stark contrast to the uniformly high activity observed in the absence of carbon monoxide (Figure 3b). The adsorbed carbon monoxide blocks sites for hydrogen adsorption and thus severely reduces the overall oxidation rate, which appears as reduced current in the SECM line scan.

(41) Damjanovic, A.; Birss, V. I.; Boudreaux, D. S. *J. Electrochem. Soc.* **1991**, *138*, 2549.
(42) Gasteiger, H. A.; Markovic, N. M.; Ross, P. N. *Catal. Lett.* **1996**, *36*, 1.
(43) Markovic, N. M.; Grgur, B. N.; Lucas, C. A.; Ross, P. N. *J. Phys. Chem. B* **1999**, *103*, 487.

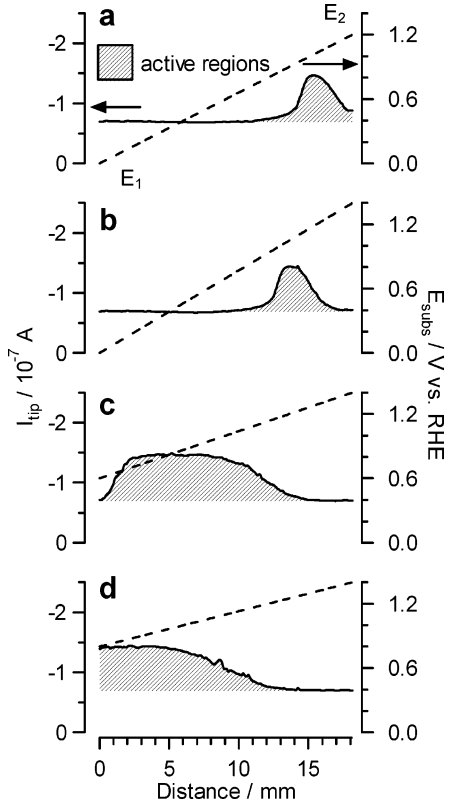

Figure 7. SECM line scans (−) over Pt-coated ITO in a CO-purged solution in the presence of various applied potential gradients (- -): (a) $E_1 = 0.0$ V and $E_2 = 1.2$ V, (b) $E_1 = 0.0$ V and $E_2 = 1.4$ V, (c) $E_1 = 0.6$ V and $E_2 = 1.4$ V, and (d) $E_1 = 0.8$ V and $E_2 = 1.4$ V. The active surface regions are denoted by the hatched pattern.

In the presence of an applied potential gradient with values spanning 0.0 and 1.4 V, several different behaviors appear in the SECM line scan (Figure 6c). At potentials between 0.0 and ∼0.8 V, a low feedback current indicates an inactive surface covered with a layer of carbon monoxide. As the potential increases above 0.8 V, the tip current increases. This reflects an activation of the platinum and coincides with the removal of carbon monoxide from the surface via oxidation. As the potential increases to more positive values, the tip current increases to a maximum near ∼1.0 V and then decreases again as the potential further increases. The increase corresponds to the removal of the carbon monoxide layer, and the decrease in current is a result of the formation of platinum oxides. A schematic of these behaviors is depicted in Figure 6d, which shows a carbon monoxide-poisoned surface at low potentials, an active zone at intermediate potentials, and an inactive zone at high potentials due to oxide formation. Notably, the region of high hydrogen oxidation activity at intermediate potential values represents a stable zone on the surface in the presence of the applied potential gradient.

The extent and location of this stable zone can be readily controlled via manipulation of the potential gradient. Figure 7 depicts several examples of SECM line scans acquired in the presence of different surface potential gradients with an adsorbed carbon monoxide layer. A decrease in the potential at E_2 to 1.2 V (Figure 7a) moves the active zone further to the right on the sample, and increasing the value of E_2 to 1.4 V (Figure 7b) moves the active zone to the left. The change in position coincides with the change in thickness of the oxide layer on the right side of the sample as the potential at E_2 is varied. The left side of the sample remains inactive as a result of the adsorbed carbon monoxide layer. Increasing the potential applied to E_1 serves to remove the carbon monoxide layer over a larger span of the surface, with the onset of high activity moving further to the left. In Figure 7c, a potential gradient between 0.6 and 1.4 V produces an expanded active zone that spans a large fraction of the surface, with only the far left side of the sample being inactive as a result of carbon monoxide and a fraction of the right side of the sample inactive as a result of oxide formation. Increasing the potential value at E_1 to 0.8 V (Figure 7d) is sufficient to remove the carbon monoxide layer completely from the sample, allowing the entire left side of the sample to be active while the far right side remains inactive as a result of oxide formation. The ability to change the applied potential gradient readily transforms the location and magnitude of the catalytically active zone on the electrode surface.

Conclusions

This work illustrates a combination of the imaging capability of the scanning electrochemical microscope with the spatial control provided by a surface potential gradient to manipulate the magnitude and spatial position of several electrochemical reactions. Examples of both catalytic and noncatalytic reactions are used to show the impact of the changing surface potential on the electrochemical reactions. These results demonstrate the unique ability of a surface potential gradient to control the magnitude and location of an electrochemical reaction on a surface. The ability to readily modify the potential gradient allows precise control over the spatial location of these reactions and the creation of stable zones of high or low reactivity on a surface. In addition, a potential gradient provides the capability of simultaneously driving an oxidation and reduction reaction on the same electrode surface. We anticipate that these features will have an impact on a range of potential analytical testing devices, particularly for microscale systems where spatial control of electrochemical phenomena provides novel control or analysis features. An example is the ability to create a well-defined, electrochemically generated pH gradient within a microscale channel for isoelectric focusing.[28] In addition, we anticipate that the spatial complexity as demonstrated with the hydrogen oxidation reaction could be exploited to study electrocatalytic reactions and to perform high-throughput catalyst screening and analysis.

Acknowledgment. We gratefully acknowledge the National Science Foundation (CTS-0405442) and Iowa State University for partial support of this work.

Supporting Information Available: Block diagram of the electronics for SECM imaging of electric field gradients. This material is available free of charge via the Internet at http://pubs.acs.org.

LA0607048